Splitting Conductors of Coils on PCB for AC-resistance Reduction

Shunsaku Nomoto, Shinjiro Shimura, Keisuke Kusaka
Dept. of Electrical, Electronics, and Information Engineering
Nagaoka University of Technology
Nagaoka, Japan
Email: s201067@stn.nagaokaut.ac.jp, kusaka@vos.nagaokaut.ac.jp

Takashi Takada
Mobility Business Development Office Automotive Company
AGC Inc.
Tokyo, Japan
Email: takashi.takada@agc.com

***Abstract*— Coils built on printed circuit boards (PCBs) have been widely used for transformers and inductors because they have the advantages of downsizing and consistency for mounting components on the PCBs. However, copper loss caused by the skin and proximity effect takes a large proportion of the total loss of the inductors at high-frequency regions. Thus, reducing copper loss is one of the significant issues for the inductors to reduce the power loss on the coils. This paper proposes a method to suppress copper loss (AC-resistance) due to the skin and proximity effect by splitting patterns of a coil and swapping them at the corner of the coil. The proposed structure for the coil is characterized as having no via, which results in an increase in cost and copper loss. The simulation results demonstrate that a 12-corner coil shape with a splitting pattern into three sections suppresses the resistance by 16.7% compared to a spiral coil and improves the quality factor by 10.9%. Practical experiments have revealed that the optimized 12-corner coil improves resistance by 24.6% and the quality factor by 18.7%.**

Keywords*— Skin effect, Proximity effect, Spiral coil, Printed circuit board (PCB)

I. INTRODUCTION

In recent years, magnetic components, such as inductors and transformers, formed using copper patterns on printed circuit boards (PCBs), have been used in certain power conversion circuits [1–7]. These magnetic components offer advantages in terms of miniaturization and ease of implementation compared to conventional windings. However, there is a problem of increased AC-resistance due to the skin and proximity effect when these magnetic components are utilized at high frequencies. In order to address this issue, some methods have been proposed to mitigate AC-resistance by arranging the patterns in a twisted configuration, similar to a litz wire [8–10].

In [8], AC-resistance is suppressed by arranging patterns of the coil such as a litz wire. However, the realization of such a structure requires a lot of vias, which may lead to increased DC resistance and complexity in implementation. In order to reduce the number of vias, a method to minimize the vias has been proposed [9]. However, in order to achieve the structure of a litz wire, the winding becomes longer, resulting in increased losses. While the structure has been proposed to suppress AC-resistance using a configuration different from that of a litz wire, there are drawbacks associated with the use of vias [10].

In order to overcome the problem mentioned above, this paper proposes new conductor pattern configurations that suppress AC-resistance without vias and the increase in length of the winding. The rest of this paper is organized as follows. First, the theory to reduce the resistance with the proposed structures is analyzed using the theoretical formula for AC-resistance due to the skin effect. Then the optimum shape to reduce the AC-resistance is discussed with a finite element method (FEM). The suppression effect of AC-resistance in the optimized coil is verified through a measurement of the prototype.

II. PROPOSED STRUCTURE OF A COIL WITHOUT VIAS

A. Skin and proximity effect of conductors

Fig. 1 illustrates the proposed pattern configurations of the coil without vias, where w and t are the width and thickness of each conductor, and c is the clearance between adjacent conductors. In order to reduce the DC resistance of the patterns, it is necessary to increase their cross-sectional area, as shown in (1)

$$R_{\mathrm{DC}} = \frac{1}{\sigma A} \tag{1},$$

where R_{DC} is the DC resistance of a conductor [Ω/m], σ is the conductivity of copper [S/m], and A is the cross-sectional area of a conductor [m^2]. However, at the higher frequencies, the skin depth δ [m] becomes smaller, as shown in (2)

$$\delta = \sqrt{\frac{1}{\pi f \mu \sigma}} \tag{2},$$

where f is the frequency [Hz], and μ is the permeability of copper [H/m], leading to an uneven distribution of current density in the conductor, increasing AC-resistance. Thus, it is necessary to split patterns to reduce AC-resistance. The total resistance for each pattern configuration is calculated using the theoretical formula for resistance due to the skin and proximity effect and verified by the effect of AC-resistance suppression. The total resistance of a conductor is composed of the conduction and proximity resistance. Each resistance is calculated by

$$R_{\mathrm{AC}} = R_{\mathrm{cond}} + R_{\mathrm{prox},x} + R_{\mathrm{prox},y} \tag{3},$$

$$R_{\text{cond}} = \frac{1}{A\sigma}\phi_{\text{cond}} \quad (4),$$

$$R_{\text{prox},x} = \frac{4\pi}{\sigma}\phi_{\text{prox},x}H_x^2 \quad (5),$$

$$R_{\text{prox},y} = \frac{4\pi}{\sigma}\phi_{\text{prox},y}H_y^2 \quad (6),$$

where R_{AC} is the total resistance of a conductor, R_{cond} is the conduction resistance including DC resistance and resistance due to the skin effect, ϕ_{cond} is the parameter representing the conduction losses depending on frequency and geometry of the conductor, H_x and H_y is the x and y direction component of the external magnetic field, $\phi_{\text{prox},x}$ and $\phi_{\text{prox},y}$ are the parameter representing the proximity losses due to the H_x and H_y, and $R_{prox,x}$ and $R_{prox,y}$ is the proximity resistance due to the proximity effect [11]. The external magnetic field is calculated as follows

$$H_{xij} = \frac{I}{2\pi n}\frac{y_i - y_j}{\left(x_i - x_j\right)^2 + \left(y_i - y_j\right)^2} \quad (7),$$

$$H_{yij} = -\frac{I}{2\pi n}\frac{x_i - x_j}{\left(x_i - x_j\right)^2 + \left(y_i - y_j\right)^2} \quad (8),$$

$$H_x = \sum_{i=1, i\neq j}^{n} H_{xij} \quad (9),$$

$$H_y = \sum_{i=1, i\neq j}^{n} H_{yij} \quad (10),$$

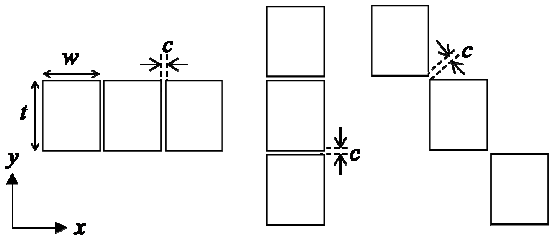

(a) Lateral (b) Vertical (c) Diagonal

Fig. 1. Configurations of patterns of a coil.

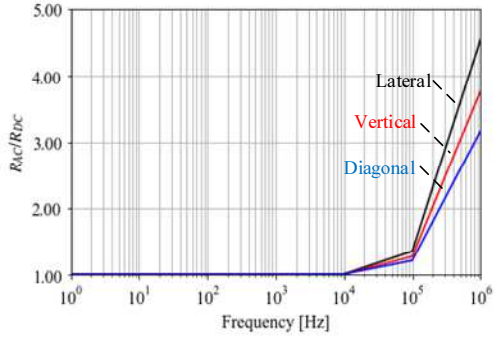

Fig. 2. AC-resistance of each configuration.

assuming that the conductors are infinitely long, where I is the current flowing through the conductor, n is the number of conductors in parallel, x_i and y_i are the center coordinates of the conductor i, and x_j and y_j are the center coordinates of the conductor j [12].

Fig. 2 shows the calculated frequency characteristics of the total resistance for each pattern, as shown in Fig. 1 with w = 0.4 mm, t = 0.5 mm, and c = 0.1 mm. From Fig. 2, it is observed that arranging the patterns diagonally, as shown in Fig. 1 (c), effectively suppresses the AC-resistance. Therefore, a structure in which patterns interchanged while maintaining the configuration was considered.

B. Proposed structure

Fig. 3 shows the proposed coil structure. Fig. 3 (b) provides an enlarged view of the pattern. When the pattern reaches the corners of the polygon, the positions of the pattern are interchanged from the inside to the outside of the coil. Importantly, since the split patterns are arranged on separate layers, no interference occurs during the interchange.

Fig. 4 and table Ⅰ show the geometric parameters of the proposed coil. This figure represents a coil with the number of splitting a pattern of three (n = 3) and five turns (n_t = 5).

III. OPTIMIZATION OF THE PROPOSED STRUCTURE

A. Consideration of the number of splitting

The parameters of the coil under consideration are presented in Table Ⅱ. In order to determine the optimal number

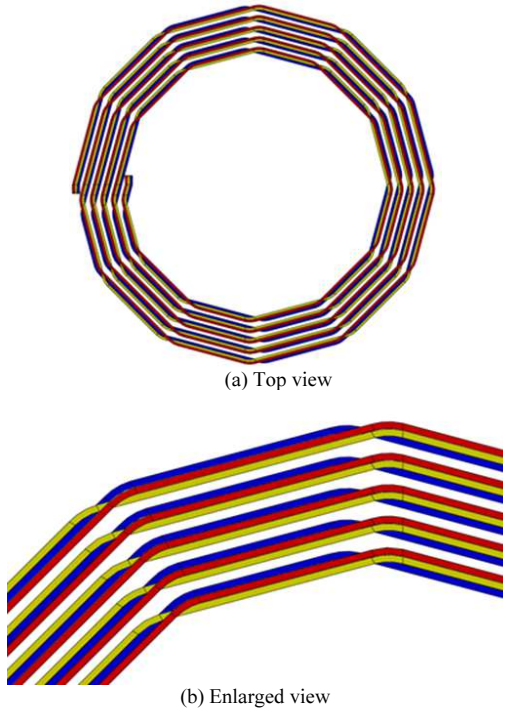

(a) Top view

(b) Enlarged view

Fig. 3. Proposed coil structure.

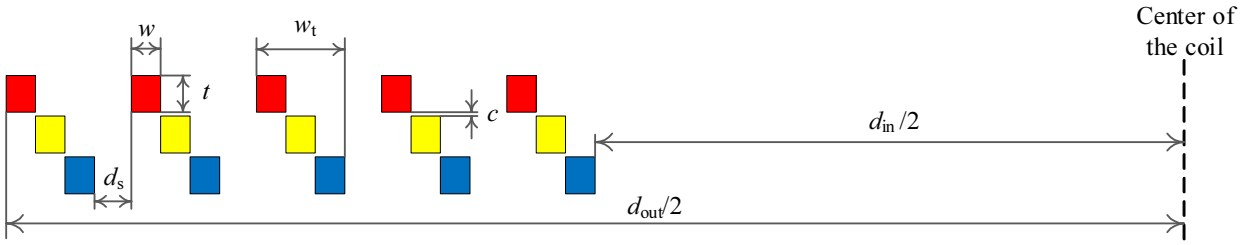

Fig. 4. Geometric parameters of the proposed coil.

of splitting that effectively suppresses the skin and proximity effect in the coil on these parameters at 100 kHz, the change in AC-resistance is analyzed through (3) while keeping the coil shape as a 12-corner polygon and varying the number of pattern divisions. In order to simplify the calculation, the pattern is assumed to be straight.

Fig. 5 shows the change in AC-resistance as the number of patterns splitting varied based on (3). From Fig. 5, the AC-resistance is most effectively suppressed when the pattern is split into three sections. Even with an increase in the number of splits of more than three sections, there is not much reduction in AC-resistance.

Based on Fig. 5, the optimal number of splits is three. However, the performance of a coil is not only determined by resistance. The coil should be evaluated considering both the resistance and inductance. Thus, the quality factor of the coil calculated by (11) is used for the comparison, where L is the inductance and R is the equivalent series resistance of the coil.

$$Q = \frac{2\pi fL}{R} \tag{11}$$

An investigation is conducted to determine the optimal number of splits with the Finite Element Method (FEM). The simulation conditions are set at the dodecagonal coil structure, as shown in Fig. 3, with a frequency of 100 kHz, and a current of 28 A. In order to simplify the FEM model, the coil was assumed to have a single winding.

Fig. 6 shows the change in AC-resistance as the number of patterns splitting varied based on the FEM. From Fig. 6, the AC-resistance is most effectively suppressed when the pattern is split into four sections. However, as the number of splits increases, the inductance decreases. Therefore, the quality factor is maximized with the patterns divided into three. Also, when the pattern is split into more than three sections, the resistance does not decrease much compared to the pattern divided into three. This is explained by the current density.

Fig. 7 shows the current distribution of the coil cross-section. As the number of splitting increases, the overall thickness increases due to the need to arrange patterns on different conductor layers, leading to the influence of the proximity effect in the thickness direction.

TABLE I. PARAMETERS OF COILS

Parameter	Symbol
Outer diameter	d_{out}
Inner diameter	d_{in}
Space of windings	d_s
Clearance of each splitting pattern	c
Total width of the winding	w_t
Thickness of each splitting pattern	t
Width of each splitting pattern	w
Number of splitting	n
Number of turns	n_t

TABLE II. PARAMETER VALUES OF COILS

Symbol	Value
d_{out}	60 mm
d_s	0.5 mm
c	0.01 mm
w_t	1.2 mm
t	0.5 mm
n_t	5

B. AC-resistance suppression effect of the proposed coil

In order to validate the AC-resistance reduction effect of the proposed coil, the proposed coil is compared with a spiral coil, which has the same parameters listed in Table II .

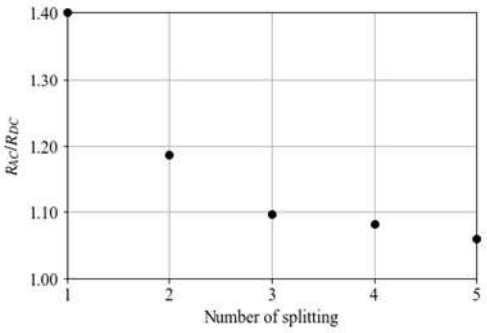

Fig. 5. Relationships between AC-resistance and split.

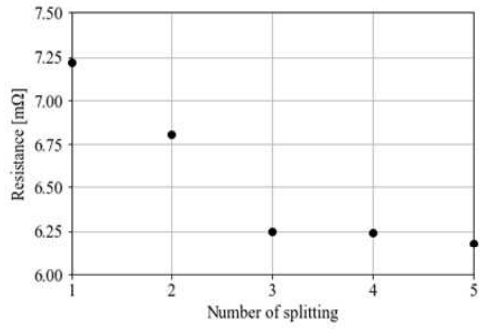

(a) Resistance

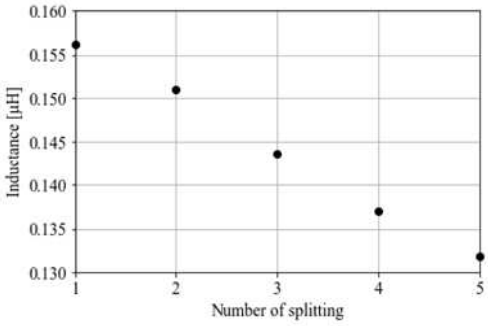

(b) Inductance

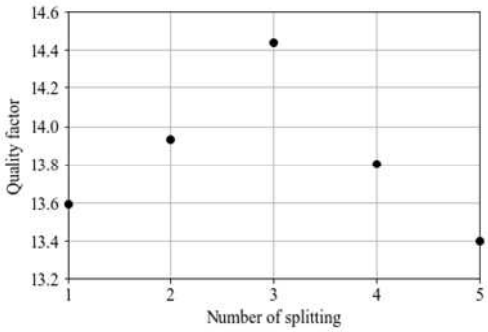

(c) Quality factor

Fig. 6. Relationships between resistance, inductance, and quality factor of the coil.

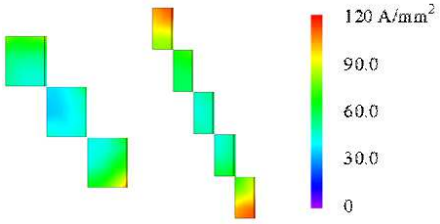

(a) 3 splits (b) 5 splits

Fig. 7. Current density distributions of the single-turn coils.

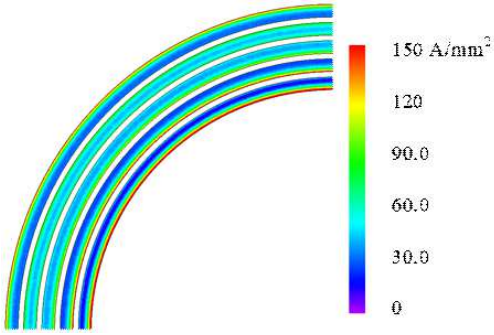

(a) Spiral

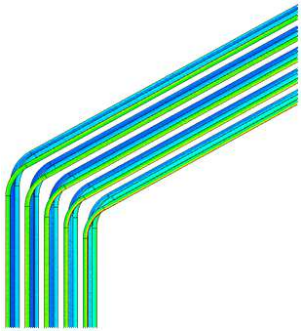

(b) 6-corner (6c)

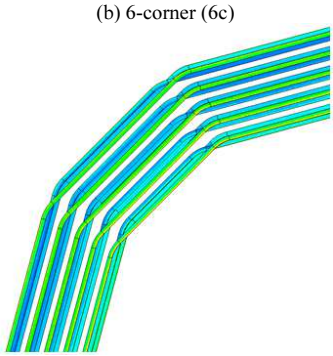

(c) 12-corner (12c)

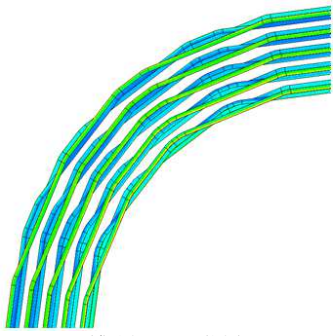

(d) 24-corner (24c)

Fig. 8. Current density distributions of the five-turn coil.

1) Current density distributions

Fig. 8 illustrates the current density distributions of the proposed coil and the spiral coil. FEM analysis is conducted with a current of 28 A and a frequency of 100 kHz. The pattern split is three based on the analysis results of the previous section. Additionally, three different shapes of the proposed coil are considered (6-corners, 12-corners, and 24-corners), for the comparison of AC-resistance.

Fig. 8 represents the current density distribution of the quarter of the coil. Since magnetic flux concentrates at the center of the coil, the current tends to bias towards the inside of the spiral coil. However, it is observed from Fig. 8 that the proposed coil exhibits less variation in current density

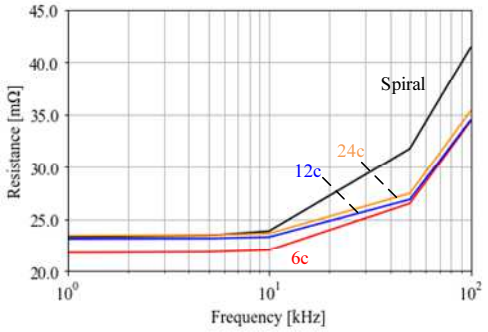

(a) Resistance

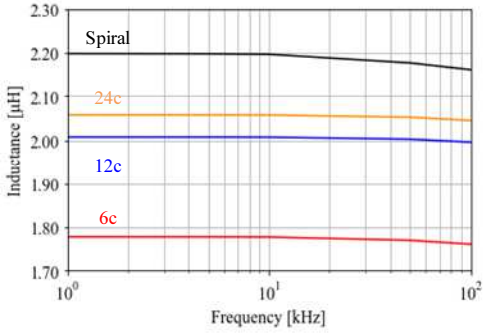

(b) Inductance

Fig. 9. Frequency characteristics of the coils.

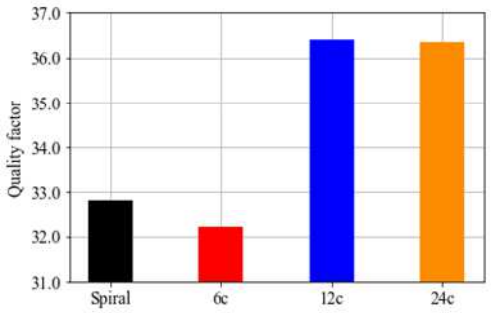

Fig. 10. Quality factor of the coils at a frequency of 100 kHz.

distribution compared to the spiral coil. Furthermore, as the number of corners in the polygon increases, the variation in the current density distribution is reduced.

2) Frequency characteristics

Fig. 9 shows the frequency characteristics of resistance and inductance for the proposed coil and the spiral coil. As the outer diameter of the spiral coil is equal to the circumscribed circle of the proposed coil, the length of the spiral coil pattern is longer than that of the proposed coil. Consequently, the resistance and inductance values of the spiral coil are larger because of the difference in pattern length. Moreover, as the number of corners in the polygon increases, approaching a circle, the difference in length decreases.

From Fig. 9 (a), the proposed coil effectively suppresses the increase of AC-resistance. Furthermore, comparing the resistance values of the proposed coil with 6c, 12c, and 24c shapes, it is evident that the 12c and 24c shapes more effectively suppress AC-resistance. At a frequency of 100 kHz, the 12c coil proposed structure achieves a reduction in resistance of at least 16.7% compared to the spiral coil.

Fig. 9 (b) shows that the inductance values of all coils remain nearly constant regardless of frequency. Additionally, as the coil shape approaches a circle, the inductance increases. This is because when the outer diameter of the coil is fixed, the inner diameter of the coil increases as the coil shape approaches a circle. As the inner diameter of the coil increases, the inductance also rises as follows,

$$L = \frac{\mu n_t^2 d_{ave}}{2}\left\{\ln\left(\frac{2.46}{\rho}\right) + 0.20\rho^2\right\} \quad (12),$$

$$d_{ave} = \frac{d_{out} + d_{in}}{2} \quad (13),$$

$$\rho = \frac{d_{out} - d_{in}}{d_{out} + d_{in}} \quad (14),$$

where d_{ave} is the average diameter and ρ is the fill ratio [13].

3) Quality factor

Fig. 10 presents the FEM analysis results of the quality factor for varying coil shapes. The quality factor of the proposed 12c coil is the highest. In comparison to the spiral coil, the 12c shape demonstrates a quality factor that is at least 10.9% higher. From this result, the optimum coil shape, which has 12 corners and three-splitting windings, is introduced, as shown in Fig. 3.

IV. Experimental Results

Fig. 11 shows prototypes of the spiral and proposed 12c coil with the common parameters listed in Table II for AC-resistance evaluation. The equivalent series resistance and inductance of these coils are measured by the LCR meter (IM3533).

A. AC-resistance

Fig. 12 shows the frequency characteristic of the AC-resistance of the coils with reference to the resistance at 1 kHz. From Fig. 12, the proposed 12c coil effectively suppresses the increase of AC-resistance at high frequencies. At a frequency of 100 kHz, the 12c coil achieves a reduction in resistance of at

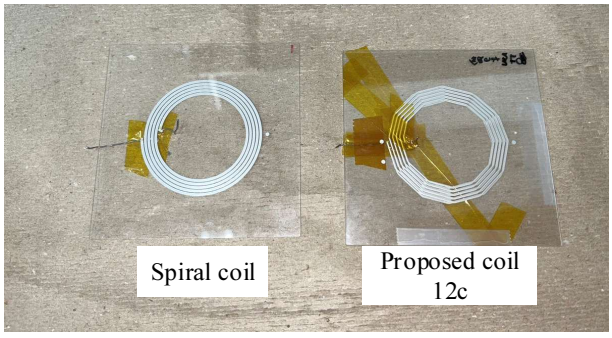

Fig. 11. Prototypes of the spiral and proposed 12c coil.

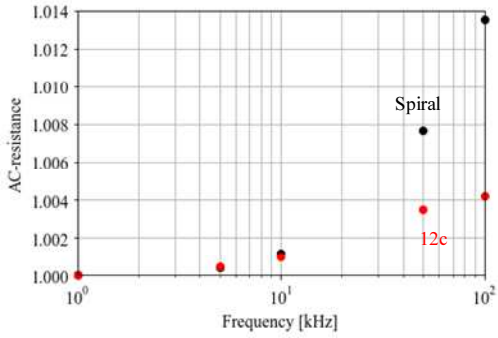

Fig. 12. Frequency characteristic of the AC-resistance of the coils.

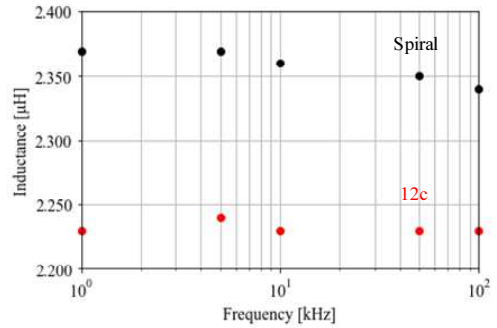

Fig. 13. Frequency characteristic of the inductance of the coils.

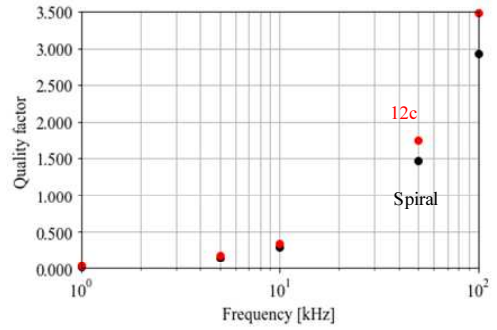

Fig. 14. Frequency characteristic of the quality factor of the coils.

least 24.6% compared to the spiral coil, where the resistance of the spiral and 12c coil at 1 kHz is 495.4 mΩ and 401.1 mΩ.

B. Inductance

Fig. 13 shows the frequency characteristic of the inductance of the coils. Fig. 13 has the same characteristics as shown in Fig. 9 (b). The inductance values of both of the coils remain nearly constant regardless of frequency.

C. Quality Factor

Fig. 14 shows the frequency characteristic of the quality factor of the coils. In comparison to the spiral coil, the 12c coil demonstrates a quality factor that is at least 18.7% higher.

V. Conclusion

This paper proposes a new coil pattern formed on printed circuit boards to suppress the AC-resistance. The proposed structure involves splitting the patterns constituting the coil in the width direction and shaping the coil into a polygon. Simulation results demonstrate that by employing a 12c coil shape and dividing the patterns into three parts, the proposed approach achieves a resistance reduction of over 16.7% compared to a spiral coil, and improves the quality factor by 10.9%, as confirmed by FEM analysis. Practical experiments have revealed that the optimized 12c coil improves resistance by 24.6% and the Q factor by 18.7%.

References

[1] J. Z. Zhang, K. Xu, Z. -W. Xu, J. Xu, X. Ren, and Q. Chen, "GaN VHF Converters With Integrated Air-Core Transformers," in IEEE Transactions on Power Electronics, vol. 34, no. 4, pp. 3504–3515, April 2019.

[2] S. R. Cove, M. Ordonez, F. Luchino, and J. E. Quaicoe, "Applying Response Surface Methodology to Small Planar Transformer Winding Design," in IEEE Transactions on Industrial Electronics, vol. 60, no. 2, pp. 483–493, Feb. 2013.

[3] L. A. R. Tria, D. Zhang, and J. E. Fletcher, "Planar PCB Transformer Model for Circuit Simulation," in IEEE Transactions on Magnetics, vol. 52, no. 7, pp. 1–4, July 2016.

[4] S. C. Tang, S. Y. Hui and H. S. . -H. Chung, "Characterization of coreless printed circuit board (PCB) transformers," in IEEE Transactions on Power Electronics, vol. 15, no. 6, pp. 1275–1282, Nov. 2000.

[5] Akihiro Konishi, Kazuhiro Umetani, Masataka Ishihara, and Eiji Hiraki, "Autonomous Resonant Frequency Tuner for a 6.78MHz Inductive Coupling Wireless Power Transfer System to Stably Maximize Repeater Current," in IEEJ Journal of Industry Applications, vol. 12, no. 2, pp. 215–227, March 2023.

[6] Keigo Arita, Yusuke Hayashi, and Kazuto Takao, "99%, 15W/cm^3 Capacitively Coupled Modular DCPET for Low-Voltage DC Power Supply Systems," in IEEJ Journal of Industry Applications, vol. 12, no. 3, pp. 401–408, May 2023.

[7] Keisuke Kusaka, Kazuki Yamagata, Jin Katsuya, and Tetsu Sato, "Reduction in Leakage Magnetic Flux of Wireless Power Transfer Systems with Halbach Coils," in IEEJ Journal of Industry Applications, vol. 12, no. 6, pp. 1104–1105, Nov. 2023.

[8] A. Narvaez, C. Carretero, I. Lope, and J. Acero, "Printed Circuit Board Coils of Multitrack Litz Structure for 3.3-kW Inductive Power Transfer System," in IEEE Transactions on Transportation Electrification, vol. 9, no. 3, pp. 3947–3957, Sept. 2023.

[9] I. Lope, J. Acero, J. Serrano, C. Carretero, R. Alonso, and J. M. Burdio, "Minimization of vias in PCB implementations of planar coils with litz-wire structure," 2015 IEEE Applied Power Electronics Conference and Exposition (APEC), pp. 2512–2517, 2015.

[10] K. Orikawa, S. Kanno and S. Ogasawara, "A Winding Structure of Air-Core Planar Inductors for Reducing High-Frequency Eddy Currents," in IEEE Transactions on Industry Applications, vol. 58, no. 6, pp. 7572–7580, Nov.–Dec. 2022.

[11] I. Lope, C. Carretero, J. Acero, R. Alonso, and J. M. Burdío, "AC Power Losses Model for Planar Windings With Rectangular Cross-Sectional Conductors," in IEEE Transactions on Power Electronics, vol. 29, no. 1, pp. 23–28, Jan. 2014.

[12] Tsutomu Mizuno, Akira Kamiya, Yusuke Shimura, Kazutaka Iida, Daisuke Yamamoto, Naoki Miyao, and Hideaki Sasadaira, "Consideration on Influences of Number of Strands on AC Resistance of Litz Wire", The Japan Society Applied Electromagnetics and Mechanics, vol. 18, no. 3, pp.124–129, 2010.

[13] S. S. Mohan, M. del Mar Hershenson, S. P. Boyd and T. H. Lee, "Simple accurate expressions for planar spiral inductances," in IEEE Journal of Solid-State Circuits, vol. 34, no. 10, pp. 1419–1424, Oct. 1999 .